

COROT week N° 3

Non-adiabatic asteroseismology and the COROT space mission

M.-A. Dupret¹, R. Scuflaire¹, R. Garrido², J. De Ridder³, C. Aerts³, P. De Cat³,
A. Moya², J. Montalbán¹, A. Noels¹, A. Thoul¹

¹ Institut d'Astrophysique et de Géophysique de l'Université de Liège, Belgium

² Instituto de Astrofísica de Andalucía - CSIC, Granada, Spain

³ Instituut voor Sterrenkunde, Katholieke Universiteit Leuven, Belgium

1. Introduction

The object of asteroseismology and one of the main goal of the COROT space mission is to improve our knowledge of the interiors of stars by using all the informations coming from their oscillations. The classical approach is to measure very precisely the pulsation frequencies of a star and, by confronting them to the theoretical predictions, to derive constraints on its internal characteristics (sound speed, density, ...). Another complementary approach, which is the object of this poster, is to derive additional constraints based on other observables: the amplitudes and phases of magnitude variations in different color filters. On one hand, these observables permit to identify the degree ℓ of the modes (Watson 1988, Heynderickx et al. 1994, Garrido 2000), which is very useful for stars whose the mode selection mechanisms are not well understood: δ Scuti, β Cephei stars, ... On the other hand, since these observables are directly linked to the photospheric layers where the pulsation is highly non-adiabatic, by confronting them to the theoretical predictions of a non-adiabatic pulsation code, constraints can be derived on the models: envelope convection, chemical composition, atmosphere models. We term this method *non-adiabatic asteroseismology*. We present here some typical results and constraints

obtained with the non-adiabatic code of Dupret for 3 types of pulsating stars: the β Cephei, the δ Scuti and the Slowly Pulsating B stars (SPB). In the EXO field of the COROT space mission, a three-color information will be available (see Sect. 6), which could be used for mode identification and non-adiabatic asteroseismology.

2. Non-adiabatic asteroseismology and Multi-color photometry

2.1 Non-adiabatic oscillations

In the superficial layers of a star, the thermal relaxation time is lower than the pulsation periods, so that the oscillations are highly non-adiabatic. In the teams of Liège and Granada, we have implemented two non-adiabatic codes with special care given to the treatment of the pulsation in the atmosphere (Dupret et al. 2002). This treatment improves significantly the accuracy of the theoretical non-adiabatic predictions. For a given model and for each modes, our non-adiabatic codes compute two basic ingredients for the confrontation with photometric observables: the amplitude f_T and the phase ψ_T of local effective temperature variation, as well as the amplitude of local effective gravity variation f_g , for a normalized radial displacement at the photosphere.

2.2 Multi-color photometry

Under some hypotheses detailed in Dupret et al. (2003): one-layer approximation, rotation-pulsation interaction neglected, . . . the monochromatic magnitude variation for the mode (ℓ, m) and wavelength λ is given by :

$$\begin{aligned} \delta m_\lambda = & -\frac{2.5}{\ln 10} \epsilon P_\ell^m(\cos i) b_{\ell\lambda} \left[(1-\ell)(\ell+2) \cos(\sigma t) \right. \\ & \left. + f_T \cos(\sigma t + \psi_T) (\alpha_{T\lambda} + \beta_{T\lambda}) - f_g \cos(\sigma t) (\alpha_{g\lambda} + \beta_{g\lambda}) \right], \end{aligned} \quad (1)$$

where ϵ is the amplitude of the radial displacement, i is the inclination angle of the star, $b_{\ell\lambda}$, $\alpha_{T\lambda}$, $\alpha_{g\lambda}$, $\beta_{T\lambda}$ and $\beta_{g\lambda}$ are defined in Balona & Evers (1999).

By integrating Eq. (1) over the passbands, we obtain quantities which can be directly confronted to the observed amplitude ratios and phase differences of photometric magnitude variations between different filters. The degree ℓ , which appears explicitly in Eq. (1) can be determined with this method.

2.3 Non-adiabatic asteroseismology

We see in Eq. (1) that the theoretical photometric magnitude variations are strongly dependent on the non-adiabatic amplitude and phase of local effective temperature variation f_T and ψ_T . Once we have identified the mode(s), and since the non-adiabatic predictions depend on the equilibrium model, we can therefore search by an iterative procedure the model which gives the best fit between the theoretical and observed photometric amplitude ratios and phase differences. The values of f_T and ψ_T computed by our non-adiabatic code depend strongly on the metallicity for β Cephei and SPB stars and on the characteristics of the very thin superficial convective zone for δ Scuti and γ Doradus stars. These characteristics (metallicity, convective zone) are generally not precisely known and not well constrained by the pulsation frequencies alone. The constraints derived from the confrontation between the observed photometric amplitudes and phases and the non-adiabatic predictions are thus more reliable in this context. We note also that the atmosphere models themselves can be constrained by this method, since the derivatives of the flux and the limb-darkening law ($\alpha_{T\lambda}$, $\alpha_{g\lambda}$, $b_{\ell\lambda}$, $\beta_{T\lambda}$ and $\beta_{g\lambda}$), directly linked to the atmosphere models, play a significant role in Eq. (1).

The stellar models used in this study were computed with the new Code Liégeois d'Evolution Stellaire (CLÉS) written by R. Scuflaire.

3. β Cephei stars

We illustrate here the application of our method to the β Cephei star EN (16) Lac, using the photometric amplitudes with Johnson filters derived by Jerzykiewicz (1993). From the amplitude ratios, we identified the degrees ℓ of the 3 frequencies $f_1 = 5.9112 \text{ c d}^{-1}$, $f_2 = 5.8551 \text{ c d}^{-1}$ and $f_3 = 5.5033 \text{ c d}^{-1}$ as $\ell = 0, 2$ and 1 , respectively. Moreover, we could constrain the metallicity of EN Lac. In figures 1 and 2, we present the results obtained for models with different metallicities and effective temperatures. The higher the metallicity, the more efficient the κ mechanism, which implies a more important decrease of the luminosity variation in the driving region and thus a smaller effective temperature variation f_T (for a normalized displacement). The best agreement between the theoretical and observed amplitude ratios was obtained for a model with $Z = 0.015$. Values below $Z = 0.015$ do not lead to excitation of the modes.

4. δ Scuti stars

We present now some applications to $2 M_\odot$ δ Scuti models with different values of the mixing length parameter α . As illustrated in Figure 3, our non-adiabatic results (mainly the phase-lag ψ_T) are very sensitive to the size of the thin superficial convection zone (linked to α), confirming the results of Balona & Evers (1999). In Figure 4, we show the results obtained in Strömngren filters phase-amplitude diagrams for two δ scuti models with $\alpha = 0.5$ (top) and $\alpha = 1.5$ (bottom). The characteristics of the thin superficial convection zone can thus be constrained by searching for the best fit between the non-adiabatic predictions and the observed amplitudes and phases.

5. Slowly Pulsating B stars

SPB stars are high order g-modes pulsators with periods between 1 and 4 days. We applied our method to 13 SPBs observed with Geneva photometry by De Cat et al. (2002). In Figure 5, we illustrate the non-adiabatic results and mode identification obtained for the star HD 74560. We see that the dominant frequency of this star ($f = 0.64472 \text{ c d}^{-1}$) is identified as an $\ell = 1$ mode. This result is in full agreement with the spectroscopic mode identification achieved with the moment method by De Cat et al. (in preparation).

6. Links with the COROT space mission

The prism of the COROT EXO field will give colored information. We emphasize that this information, expressed in term of amplitude ratios and phase differences, could be used for mode identification and non-adiabatic asteroseismology, as described above. With the COROT prism, the wavelengths corresponding to the 3 colors will intrinsically depend on the effective temperatures of the targets, contrary to filters with constant passbands. This needs a special expertise that we are developing in collaboration with the team of Rafael Garrido. We refer to the posters of Montalban et al. and Barban et al. (this conference), which are closely linked to this project.

References

- Balona, L.A., Evers, E.A., 1999, MNRAS 302, 349
- De Cat, P., and Aerts, C., 2002, A&A 393, 965
- Dupret, M.-A., De Ridder, J., Neuforge, C., Aerts, C., and Scufflaire R., 2002, A&A 385, 563
- Dupret, M.-A., De Ridder, J., De Cat, P., Aerts, C., Scufflaire, R., Noels, A., Thoul, A., 2003, A&A, in press
- Garrido, R., 2000, In: The 6th Vienna Workshop on δ Scuti and related stars,

eds. M. Montgomery, M. Breger, PASP Conference Series, 210, 67

Garrido, R., Garcia-Lobo, E., Rodriguez, E., 1990, A&A 234, 262

Heynderickx, D., Waelkens, C., Smeyers, P., 1994, A&AS 105, 447

Jerzykiewicz, M., 1993, Acta Astron. 43, 13

Watson, R.D., 1988, Ap&SS 140, 255

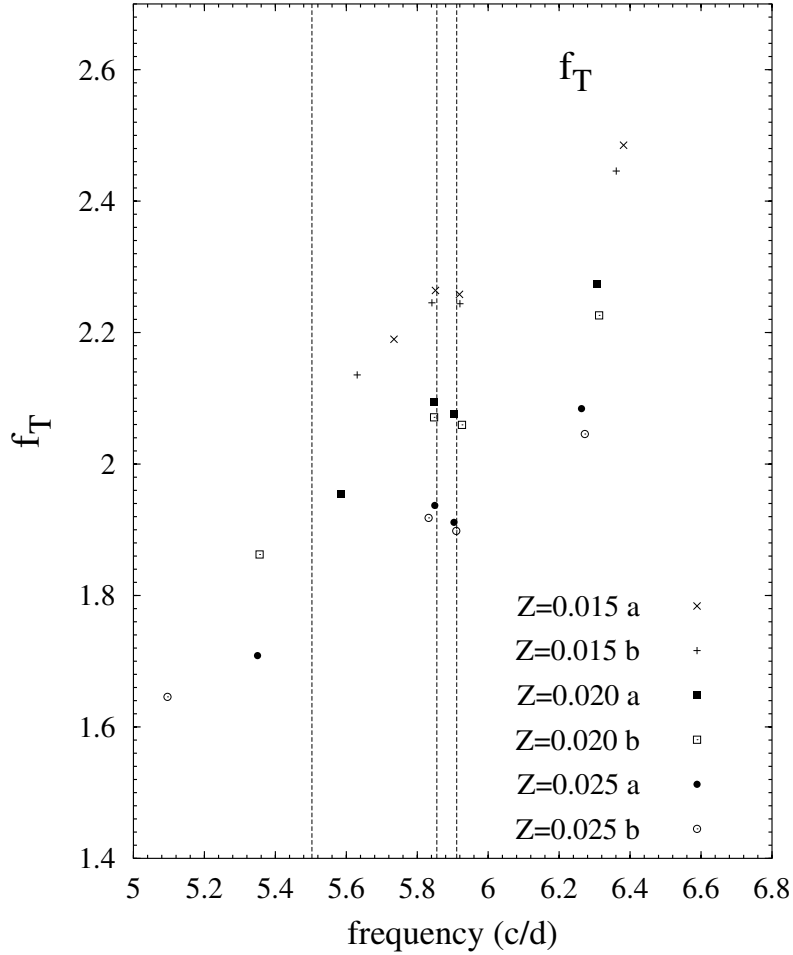


Figure 1: f_T (defined in Sect. 2.1) as function of the frequency in c d^{-1} , for different modes ($0 \leq \ell \leq 2$) and for six different models of the star EN Lac with 3 different metallicities. For each metallicity, two values of the effective temperature have been chosen: the models a (colder) and the models b (hotter). The three vertical lines correspond to the three observed frequencies.

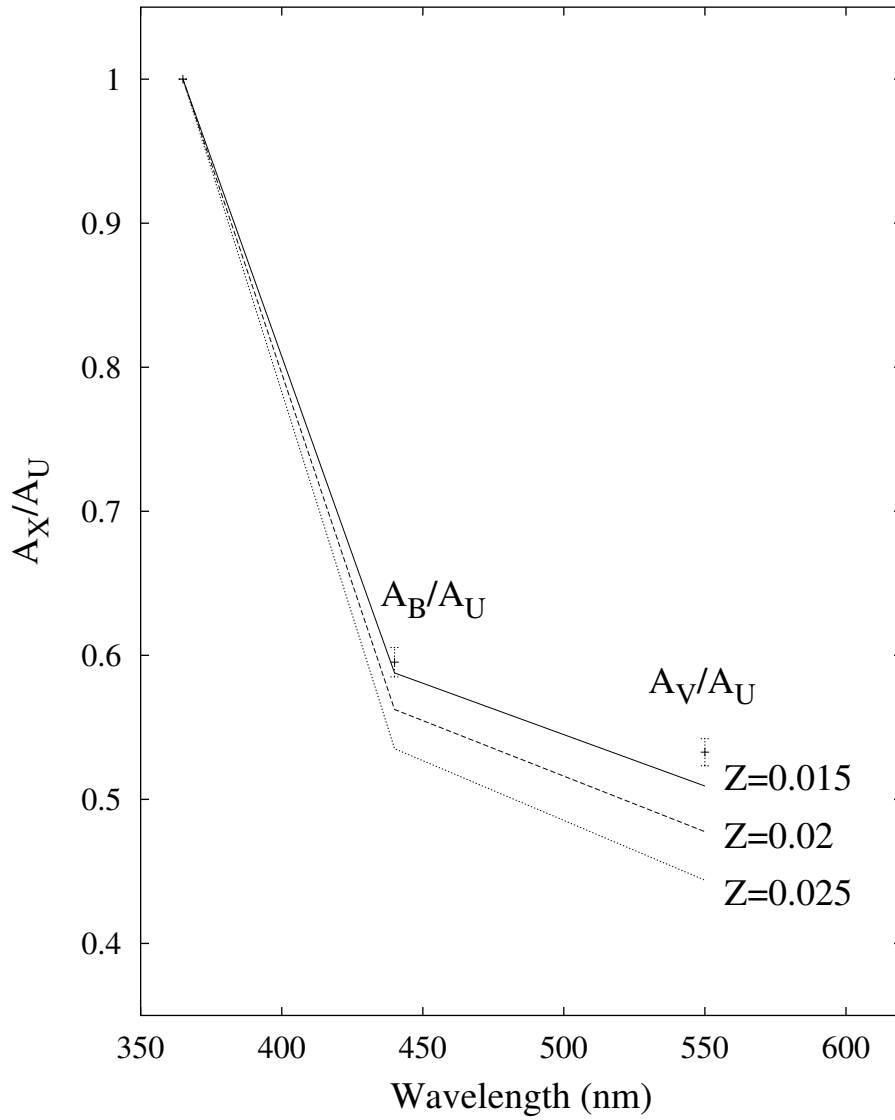


Figure 2: Observed amplitude ratios (error bars) and theoretical ones (lines) with Johnson photometry, for the radial p_1 mode obtained for three models of EN Lac with different metallicities.

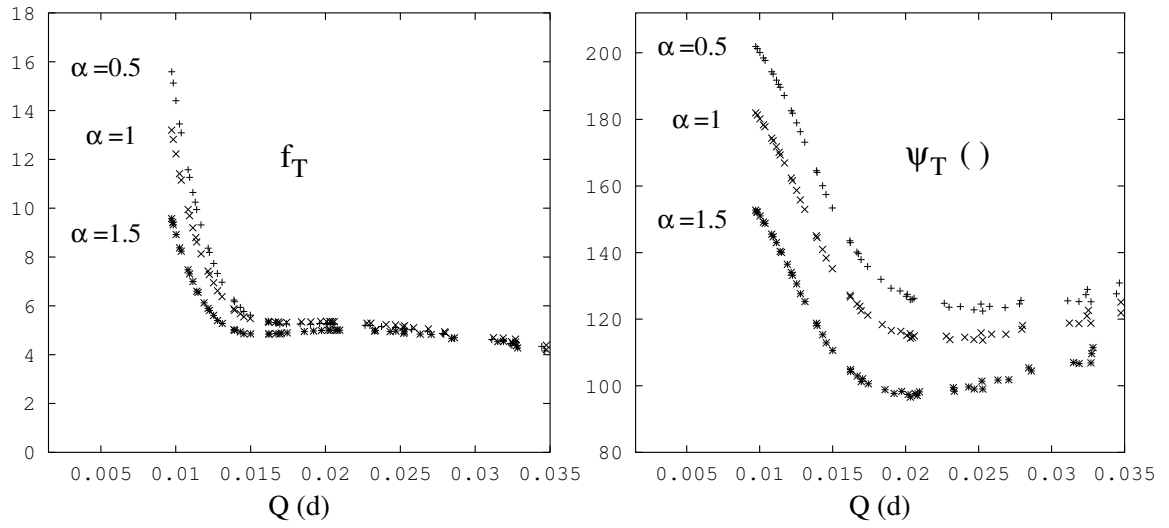


Figure 3: Non-adiabatic effective temperature variations f_T (left) and phase-lags ψ_T (right) as function of the constant of pulsation Q in days, for different modes of $2 M_\odot$ δ Scuti models with different values of α (0.5, 1 and 1.5). The “+” are for the model with $\alpha = 0.5$, the “ \times ” for the model with $\alpha = 1$ and the asterisks for the model with $\alpha = 1.5$.

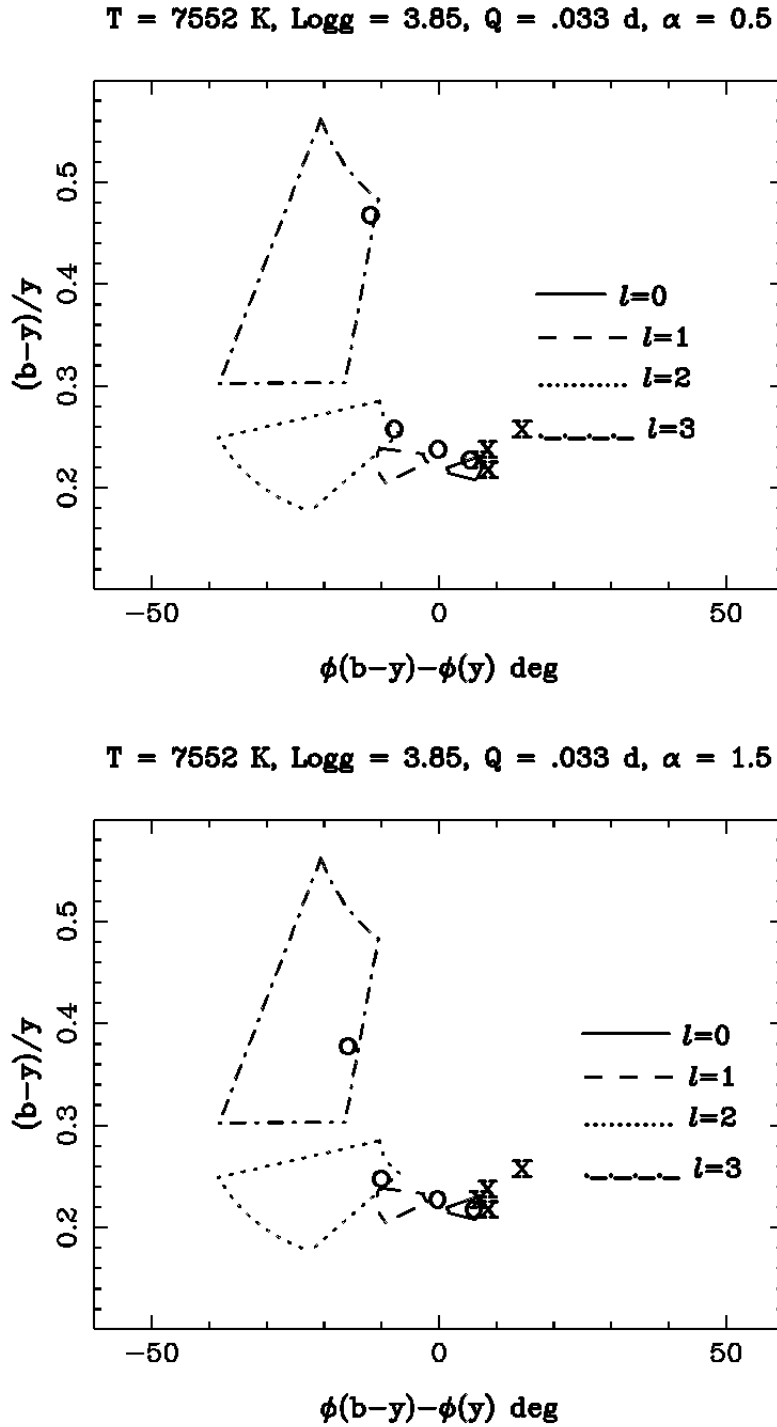


Figure 4: Strömgren filters phase-amplitude diagrams for two δ Scuti models with $\alpha = 0.5$ (top) and $\alpha = 1.5$ (bottom). The different regions are for different degrees ℓ and correspond to the old method where the degree of non-adiabaticity R and the phase-lag ψ_T were free parameters (Garrido et al. 1990). The circles are our non-adiabatic predictions for modes with frequencies closest to the fundamental radial one ($Q \simeq 0.033 \text{ d}$); and the crosses correspond to the observations of radial pulsators.

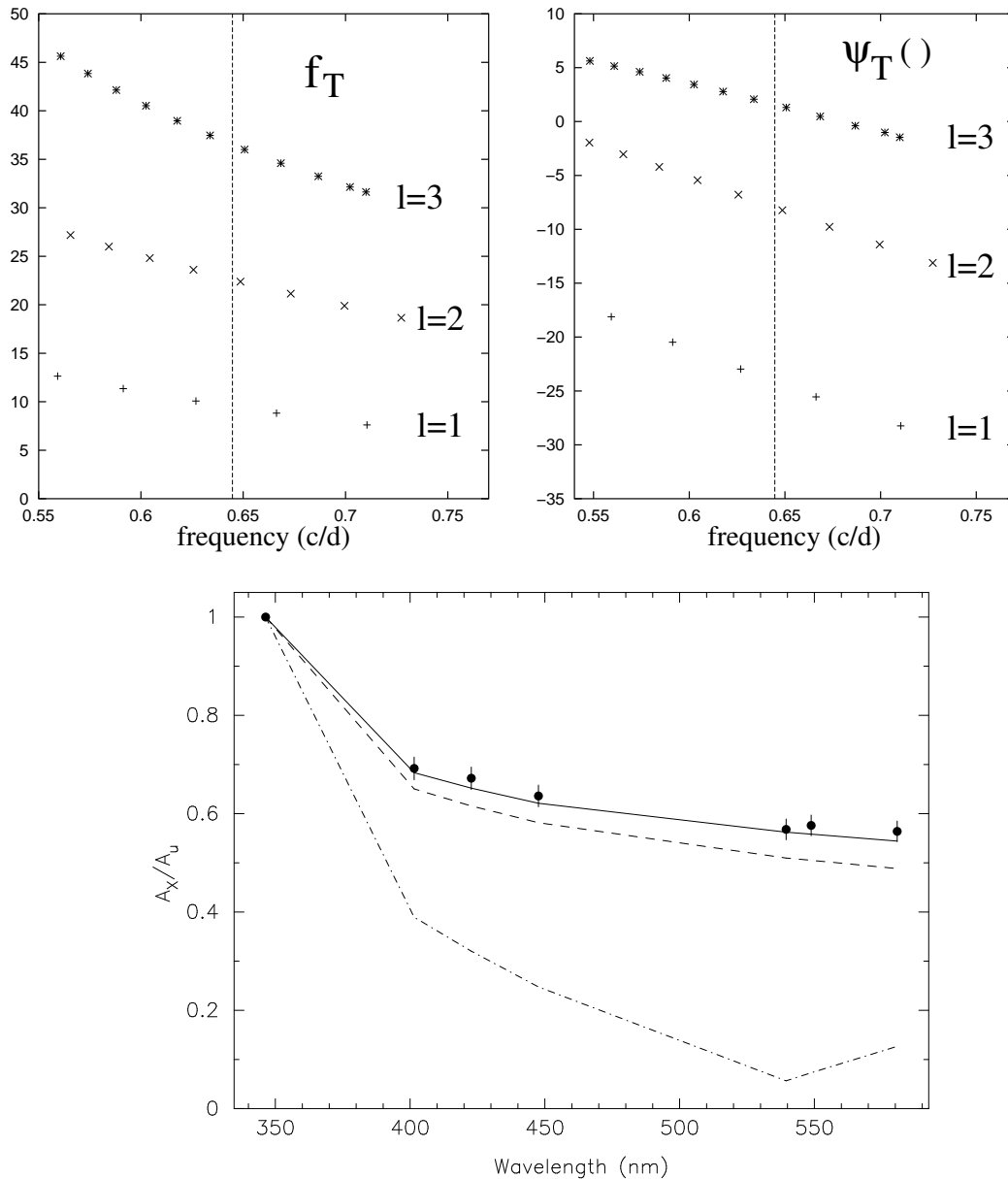


Figure 5: Model calculations for the SPB star HD 74560. Non-adiabatic values of f_T on the top left panel and ψ_T on the top right panel (defined in Sect. 2.1), as function of the pulsation frequency in c/d. On the bottom panel, observed amplitude ratios (bullets) and theoretical predictions (solid line for $\ell = 1$, dashed line for $\ell = 2$ and dot-dashed line for $\ell = 3$).